The CHAP domain of Cse functions as an endopeptidase that acts at mature septa to promote Streptococcus thermophilus cell separation

Séverine Layec, Joëlle Gérard, Valérie Legué, Marie-Pierre Chapot-Chartier, Pascal Courtin, Frédéric Borges, Bernard Decaris, Nathalie N. Leblond-Bourget

molecular microbiology

The CHAP domain of Cse functions as an endopeptidase that acts at mature septa to promote S. thermophilus cell separation.

Journal:	*Molecular Microbiology*
Manuscript ID:	MMI-2008-07980.R1
Manuscript Type:	Research Article
Date Submitted by the Author:	n/a
Complete List of Authors:	Layec, Séverine; Nancy University, Genetic and Microbiology Gérard, Joelle; Nancy University, Genomic, ecophysiology and functional ecology Legué, Valérie; Nancy University, Genomic, ecophysiology and functional ecology Chapot-Chartier, Marie-Pierre; INRA, Bacterial Biochemistry Courtin, Pascal; INRA, Bacterial Biochemistry Borges, Frédéric; ENSAIA, LSGA Decaris, Bernard; Nancy University, Genetic and Microbiology Leblond-Bourget, Nathalie; Nancy University, Genetic and Microbiology
Key Words:	peptidoglycan hydrolase, Streptococcus thermophilus, cell separation, mature septa , CHAP domain

The CHAP domain of Cse functions as an endopeptidase that acts at mature septa to promote *Streptococcus thermophilus* cell separation.

Séverine Layec [1], Joëlle Gérard [2], Valérie Legué [2], Marie-Pierre Chapot-Chartier[3], Pascal Courtin[3], Frédéric Borges [1f], Bernard Decaris [1] and Nathalie Leblond-Bourget [1]*

[1]Laboratoire de Génétique et Microbiologie, UMR INRA/UHP 1128, IFR 110, Nancy-Université, BP 239, 54506 Vandoeuvre-lès-Nancy, France.

[f] present address: LSGA- Laboratoire de Science et Génie Alimentaire, ENSAIA-INPL, BP172, 54506 Vandoeuvre-lès-Nancy, France.

[2]Génomique, Ecophysiologie et Ecologie Fonctionnelles, « Interaction Arbres/Micro-organismes », UMR INRA/UHP 1136, IFR 110, Nancy-Université, BP239, 54506 Vandoeuvre-lès-Nancy, France.

[3]INRA, UR477 Biochimie Bactérienne, F-78350 Jouy-en-Josas, France

*Corresponding author : Phone: (33) 3 83 68 42 10

Fax : (33) 3 83 68 44 99

E-mail : bourget@nancy.inra.fr

Keywords: CHAP domain; cell wall hydrolase; mature septa; daughter cell separation; *S. thermophilus*

SUMMARY

Cell separation is dependent on cell wall hydrolases that cleave the peptidoglycan shared between daughter cells. In *Streptococcus thermophilus*, this step is performed by the Cse protein whose depletion resulted in the formation of extremely long chains of cells. Cse, a natural chimeric enzyme created by domain shuffling, carries at least two important domains for its activity: the LysM expected to be responsible for the cell wall-binding and the CHAP domain predicted to contain the active center. Accordingly, the localization of Cse on *S. thermophilus* cell surface has been undertaken by immunogold electron and immunofluorescence microscopies using of antibodies raised against the N-terminal end of this protein. Immunolocalization shows the presence of the Cse protein at mature septa. Moreover, the CHAP domain of Cse exhibits a cell wall lytic activity in zymograms performed with cell walls of *Micrococcus lysodeikticus*, *Bacillus subtilis* and *S. thermophilus*. Additionally, RP-HPLC analysis of muropeptides released from *B. subtilis* and *S. thermophilus* cell wall after digestion with the CHAP domain shows that Cse is an endopeptidase. Altogether, these results suggest that Cse is a cell wall hydrolase involved in daughter cell separation of *S. thermophilus*.

INTRODUCTION

Cell separation can be defined as the mechanism needed to disconnect the two new daughter sacculi after the cell division is completed (or at the very late step of cell division). This is still a poorly understood process that requires the involvement of cell wall hydrolases. Cell-separating hydrolases were mostly identified by phenotypic analysis, their absence resulting in the formation of chains of unseparated cells (Borges *et al.*, 2005; Buist *et al.*, 1995; Fukushima *et al.*, 2006; Garcia *et al.*, 1999; Heidrich *et al.*, 2001; Margot *et al.*, 1998; Margot *et al.*, 1999; Yoshimura *et al.*, 2006) or in a highly aggregated phenotype (Kajimura *et al.*, 2005). In *Streptococcus thermophilus*, the deletion of *cse* led to a dramatic increase of the chain length indicating that Cse is the key *S. thermophilus* cell-separating enzyme (Borges *et al.*, 2005).

The Cse protein consists of four regions: a signal peptide and a LysM domain at its N-terminus, a catalytic domain at its C-terminus, both domains being separated by a central variable region (Borges *et al.*, 2005; Borges *et al.*, 2006). The LysM motif functions as a general peptidoglycan binding module (Eckert *et al.*, 2006; Steen *et al.*, 2005a) that may play important roles in appropriate localization and/or recognition of substrates (Fukushima *et al.*, 2006; Kajimura *et al.*, 2005; Steen *et al.*, 2005a; Yamamoto *et al.*, 2003).

The C-terminal catalytic domain of Cse carries a Cysteine, Histidine-dependent Amidohydrolases/Peptidases (CHAP) domain conferring to the protein a potential catalytic activity (Borges *et al.*, 2005; Layec *et al.*, 2008a). Point mutation of the conserved Cys and His residues or total deletion of this domain reveals that it retains cell wall hydrolase activity (Donovan *et al.*, 2006; Navarre *et al.*, 1999; Nelson *et al.*, 2006; Pritchard *et al.*, 2004; Yokoi *et al.*, 2005).

Among the *Firmicutes*, few bacterial and phage-encoded CHAP proteins have been characterized and participate either in cell division (Chia *et al.*, 2001; Mattos-Graner *et al.*, 2006; Ng *et al.*, 2004; Reinscheid *et al.*, 2001) daughter cell separation (Borges *et al.*, 2005; Kajimura *et al.*, 2005) or in cell lysis (Donovan *et al.*, 2006; Huard *et al.*, 2003; Navarre *et al.*, 1999; Pritchard *et al.*, 2004; Yokoi *et al.*, 2005).

By analogy with other cell-separating enzymes and taking into account the involvement of Cse in cell disconnection, we postulate that Cse is a cell wall hydrolase probably acting at cell separation sites. However, there has been no direct evidence concerning either the Cse catalytic activity or its localization at the *Streptococcus thermophilus* cell surface. In this study, we provide genetic and biological evidence that Cse separates daughter cells by cleaving the bond between D-Ala of the stem peptide and L-Ala of the cross-bridge in *S. thermophilus* peptidoglycan at mature septa.

RESULTS

The LysM and CHAP domains are essential for Cse cell separating activity.

To get more insight into the biological role of the LysM and CHAP domains of the Cse protein, in frame deletion mutants were constructed resulting in the cseΔLysM and cseΔCHAP mutant strains (Fig. 1A). Semi-quantitative RT-PCR was used to quantify the level of expression of *cse* alleles in the wild-type and the mutant strains. The level of expression of *gyrA* was included an internal housekeeping control to ensure that equivalent amounts of RNA were used for the RT-PCR analysis. As shown in Fig. 1B, there is no significant difference between the levels of expression of the different alleles.

Visual inspection of overnight standing HJL cultures revealed that turbidity in the cultured medium was only observed for the CNRZ368 control strain whereas the cells of the Δcse, cseΔLysM and cseΔCHAP mutants all flocculate at the bottom of the tube (Fig. 2A). To determine if the sedimentation properties of these mutants correlate with an increase of their chain length, aliquots of each culture were observed under light microscopy followed by the counting of the number of cells per chain. As observed in Fig. 2B, chains of the wild-type strain were rather small since 70% of them were constituted by less than 40 cells. By contrast, chains of the 3 *cse* deletion mutants were mostly composed of more than 201 cells. Complementation experiments were performed by transformation of the cseΔLysM and cseΔCHAP mutants with pNST260^{+}::*cse*, a vector containing an intact copy of *cse* that we developed previously (Borges *et al.*, 2005). Complemented strains exhibited a wild-type phenotype with respect to the number of cells per chain and to the sedimentation property while the negative control maintained a mutant phenotype (data not shown). Thus, deletion of the LysM or the CHAP domain of the *cse* gene had a clear effect on the chain length indicating that both domains were required for Cse efficient cell separation activity.

Cse is involved in late stage of cell division.

Transmission electron microscopy of both the wild-type and the Δcse mutant revealed that they formed linear chains that appeared like linear necklaces of diplococcal cells (Fig. 3). As observed for *S. pneumoniae* (Morlot *et al.*, 2003), progression of the *S. thermophilus* septum synthesis is materialized by three kinds of septa (Fig. 3C and F): (i) nascent septum (a) located equidistant from the cell poles and initiated by the constriction ring, (ii) intermediate septum (b) generated by further constriction of the cell walls and (iii) mature septum (c) observed at the end of the division process and corresponding to an extension of the septum holding daughter cells together. No impairment of the septum formation was observed in the Δcse mutant suggesting that Cse had no role in cell wall synthesis at septa. The only difference between the Δcse mutant (Fig. 3A to C) and the wild-type strains (Fig. 3D to F) is the regularity of the cell morphology. Within the mutant, the chains of cells consist of a regular succession of diplococcus, a phenotype that corresponds to fully divided cells. A more irregular phenotype is observed in the wild-type suggesting that the processes of cell division and of disconnection of daughter cells could interfere.

Since deletion of *cse* led to a dramatic reduction of daughter cell separation and because the material linking daughter cells was expected to be peptidoglycan, we postulate that Cse acts as a late cell wall hydrolase that is able to bind *S. thermophilus* cell surface and separate divided cells.

Localization of Cse and its derivatives at *S thermophilus* cell surface.

In a previous study, we demonstrate that Cse is an extracellular protein whose export is signal peptide dependent (Borges *et al.*, 2005). Moreover, a search of the Conserved Domain Database shows that the N-terminal parts of Cse contain a LysM domain potentially involved in Cse attachment to the cell wall. Thus, to visualize the specific localization of Cse on the *S. thermophilus* cell surface, we utilized immunogold electron microscopy. To avoid the simultaneous detection of Cse and PcsB sharing the same C-terminal end (Borges *et al.*, 2005), antibodies were raised against a specific region (from 1 to 183 aa) of the Cse protein. As shown in Fig. 4, the labelled gold particles were localized on the fine link connecting daughter cells and within adjacent cell poles

(Fig. 4A and B). However, because of the darkness of the cells, we could not determine if labelled particles were present elsewhere. We used next immunofluorescence microscopy on the wild-type strain, and confirmed that Cse binding was highly localized at mature septa with no or little Cse protein at nascent septa (Fig. 5A2 and E2). Staining of the wild-type *S. thermophilus* cells with calcofluor fluorescent dye (Fig. 5, E4) which stains cell walls blue confirmed the specific binding of Cse to the peptidoglycan of the mature septa. No fluorescence was detected on the cseΔlysM mutant (Fig. 5C) or on the wild-type strain stained with preimmue serum (Fig. 5B) used as negative controls. Fluorescence analysis of the cseΔVar and cseΔCHAP mutants (Fig. S1C and Fig. 5D) showed that the Cse derivatives were capable of recognizing the same targets but surprisingly the patterns of fluorescence was more diffuse than that of the wild-type strain.

Cse is an endopeptidase.

(i) The CHAP domain of Cse confers the cell wall hydrolytic activity.

In a previous study, we tried to overexpress the full length Cse protein but our attempts failed. This time, only the CHAP domain of Cse (from position in aa 341 to 461) was expressed in *E. coli*. To facilitate the purification of the CHAP protein, a hexa-histidine tag was introduced at its N-terminus. On SDS-PAGE, the purified CHAP-His_6-tagged protein gave a band of about 15 kDa estimated to be more than 96% pure (Fig. S2). This band corresponded to the cell-wall hydrolyzing band observed on zymogram and was also revealed by Western immunoblot analysis using an anti-His tag monoclonal antibody (Fig. S2). Zymograms were done using as substrates cells from *Micrococcus lysodeikticus* (data not shown), purified peptidoglycan from *B. subtilis* 168 HR (Fig. S2 and Fig. 6A) and from *S. thermophilus* Δcse mutant (Fig. S2 and Fig. 6B) and revealed that the CHAP domain carries a cell wall hydrolytic activity. The CHAP-His_6-tagged protein activity was revealed with incubation buffer containing 0.2% Triton_X100 at pH 4.0 or pH 4.5. No activity was detected at other pH (data not shown).

(ii) Determination of the hydrolytic specificity of the CHAP domain of Cse on *B. subtilis* peptidoglycan.

In the literature, the CHAP domain of several phage-encoded lytic proteins displays an endopeptidase activity (Baker *et al.*, 2006; Donovan *et al.*, 2006; Navarre *et al.*, 1999; Nelson *et al.*, 2006; Pritchard *et al.*, 2004; Yokoi *et al.*, 2005), but this domain is also reported to function as *N*-acetylmuramoyl-L-alanine amidase (Kajimura *et al.*, 2005; Llull *et al.*, 2006). To determine the hydrolytic specificity of Cse, the purified CHAP-His_6-tagged protein was used to digest purified peptidoglycan of *B. subtilis* whose structure was established previously (Atrih *et al.*, 1999). After incubation, the digestion mixture was centrifuged and both soluble and insoluble materials were analyzed. No muropeptide or peptide could be detected in the soluble material when analyzed by RP-HPLC (data not shown) whereas an *N*-acetylmuramoyl-L-alanine amidase is expected to release peptide moieties from peptidoglycan as observed previously (Bourgeois *et al.*, 2009), this suggests that Cse does not present such specificity. The insoluble material was further digested with mutanolysin and the digestion products were analyzed by RP-HPLC. Comparison of the muropeptide profile of the peptidoglycan double digest with the muropeptide profile obtained by mutanolysin digestion of *B. subtilis* peptidoglycan (Fig. 6A), revealed a large increase of monomers in parallel with a clear decrease of dimers and trimers in the CHAP-His6-tagged protein treated sample. Especially, the amount of the major dimers, peaks 2 and 3, decreased strikingly in *B. subtilis* peptidoglycan treated with the CHAP-His_6-tagged protein whereas the amount of several monomers in peaks 1, 4 and 5, increased clearly (Fig. 6A). These results indicate that Cse CHAP-domain is able to cleave bonds inside insoluble native *B. subtilis* peptidoglycan. Cleavages occur most probably inside the peptide moieties since the decrease of dimers and trimers is accompanied with an increase of monomers suggesting that the Cse CHAP-domain has endopeptidase activity (Table 1, Fig. 6A).

(iii) Determination of CHAP hydrolytic bond specificity on *S. thermophilus* peptidoglycan.

We then characterized further the hydrolytic bond specificity of Cse CHAP-domain on muropeptides derived from *S. thermophilus* peptidoglycan by mutanolysin digestion. Peptidoglycan was digested by mutanolysin and the resulting digestion products were separated by RP-HPLC. Three muropeptides characterized by MALDI-TOF mass spectrometry (Table 1, peaks 8, 9, 10 and Fig. S3) and purified by RP-HPLC (Fig. S4) were digested with the CHAP-His_6-tagged protein to determine its cleavage site on *S. thermophilus* peptidoglycan. The resulting digestion products were analyzed by RP-HPLC. In Fig. 6B, the peaks with the highest retention times [peak 8 in (a) ; peak 9 in (b) and peak 10 in (c)] correspond to the intact muropeptides indicating partial digestion. However, the others peaks [peak 6 in (a); peaks 6 and 7 in (b) and peaks 6 to 9 in (c)] are consistent with being the CHAP-His_6-tagged protein digestion products. According to the retention times of each peak and their masses determined by MALDI-TOF MS (Table 1), muropeptide structures were proposed (Fig. S3). These results indicate that the CHAP-His_6-tagged protein cleaved the peptidic bond between the D-Ala residue of the stem peptide and the L-Ala residue of the cross-bridge of *S. thermophilus* peptidoglycan (Fig. 6B). Thus, Cse has D,L-endopeptidase activity on *S. thermophilus* peptidoglycan.

DISCUSSION

Within the *Firmicutes*, only a few CHAP proteins have been characterized that function as cell wall hydrolases. Among them are PcsB/GbpB from *Streptococcus* involved in cell division (Chia *et al.*, 2001; Mattos-Graner *et al.*, 2006; Ng *et al.*, 2004; Reinscheid *et al.*, 2001), Sle1 from *Staphylococcus aureus* (Kajimura *et al.*, 2005) and Cse from *S. thermophilus* that are necessary for daughter cell separation (Borges *et al.*, 2005). AcmB from *Lactococcus lactis* contributes to cellular autolysis (Huard *et al.*, 2003). Six other phage-encoded CHAP proteins are involved in bacterial cell lysis (Donovan *et al.*, 2006; Llull *et al.*, 2006; Navarre *et al.*, 1999; Nelson *et al.*, 2006; Pritchard *et al.*, 2004; Rashel *et al.*, 2008; Yokoi *et al.*, 2005). Besides the variety of their roles, these proteins differ by the cleavage specificity of their CHAP domains that present either an endopeptidase or an *N*-acetylmuramoyl-L-alanine amidase activity.

The CHAP domains of the ϕ11, ϕ12, B30, LysWMY and Cse proteins (Donovan *et al.*, 2006; Navarre *et al.*, 1999; Pritchard *et al.*, 2004; Sass and Bierbaum, 2007; Yokoi *et al.*, 2005) and potentially that of AcmB have an endopeptidase activity (Huard *et al.*, 2003). Alternatively, the CHAP domain of the Sle1 and Skl proteins were demonstrated to function as *N*-acetylmuramoyl-L-alanine amidase (Kajimura *et al.*, 2005; Llull *et al.*, 2006). This indicates that there is no correlation between the cleavage specificity of the CHAP proteins and their biological functions.

In a previous study, the C-terminal end of Cse, including the CHAP domain, was demonstrated to be homologous with that of PcsB/GbpB (Borges *et al.*, 2005). Many attempts were done to demonstrate the potential cell wall hydrolytic activity of these enzymes, but all failed (Borges *et al.*, 2005 ; Ng *et al.*, 2004; Reinscheid *et al.*, 2001). This time, by over expressing the CHAP domain of Cse and by searching for optimal experimental conditions, we succeeded to demonstrate its endopeptidase activity. By zymogram, Cse activity was only detected at pH 4 - 4.5. Such low pH could exist in the cell wall matrix if we consider that like *B. subtilis* (Calamita *et al.*, 2001), the cell wall of *S. thermophilus* could be protonated during growth.

The process of daughter cell separation can be view as an active process that takes place at the end or after the completion of the cell division process. Indeed, cells lacking cell-separating enzymes are inhibited only in cell separation and are not inhibited in cell division, with normal septa still being formed (Ohnishi *et al.*, 1999)**.** The cell separation process requires dedicate cell wall hydrolases that cleave the sacculi connecting daughter cells. In their vast majority, cell-separating enzymes are composed of a unique CHAP, NLPC/P60 or Glucosaminidase (more rarely Glyco_hydro_25) catalytic domain (Layec *et al.*, 2008b). The catalytic domain diversity is correlated with the diversity of the peptidoglycan linkage that they cleave. For instance, AcmA from *L. lactis* (Buist *et al.*, 1995; Steen *et al.*, 2005a) and LytB from *S. pneumoniae* (De Las Rivas *et al.*, 2002; Garcia *et al.*, 1999) carry a glucosaminidase domain conferring the *N*-acetylglucosaminidase activity. Ami A, B and C from *E. coli* and Sle1 from *S. aureus* are *N*-acetylmuramoyl-L-alanine amidases. Aml from *S. mutans*, carrying a "Glyco_hydro_25" domain, presents a *N*-acetylmuramidase activity (Yoshimura *et al.*, 2006). At last, several cell-separating enzymes display an endopeptidase activity. That is the case of Cse from *S. thermophilus* (this study) and of LytE, LytF and CwlS (YolJ) from *B. subtilis* (Fukushima *et al.*, 2006; Margot *et al.*, 1998; Margot *et al.*, 1999). Collectively, all these data clearly show that evolution has selected several alternative enzymes exhibiting distinct catalytic activity to perform the daugther cell separation process.

All the cell-separating enzymes described so far are cell surface proteins and Cse does not escape this rule. Cse is thought to bind peptidoglycan via its LysM domain. The LysM domain is one of the most common attachment modules in bacterial cell-separating enzymes. Thus, AcmA from *L. lactis*, AltA from *E. faecalis*, Sle1 from *S. aureus*, LytE, LytF and CwlS from *Bacillus* contain 2 to 6 tandem repeats of the LysM motif (Eckert *et al.*, 2006; Fukushima *et al.*, 2006; Ishikawa *et al.*, 1998; Kajimura *et al.*, 2005; Margot *et al.*, 1998; Margot *et al.*, 1999; Ohnishi *et al.*, 1999; Steen *et al.*, 2003). In addition to its role in cell wall-binding, LysM is important for biological functioning (Buist *et al.*, 2008). The chaining phenotype of the cseΔlysM mutant

corroborated these results since LysM was found to be necessary for efficient Cse cell-separating activity.

The location of only a few cell-separating enzymes has been studied so far but reveals that all of them are positioned only at cell separation sites (Fukushima *et al.*, 2006; Kajimura *et al.*, 2005; Steen *et al.*, 2003) and questions about the reasons leading to such exclusive location.

In the case of Cse, one explanation is to consider that the restricted binding of the enzyme would be ensured by its LysM domain. Another possibility is to consider that a specific mechanism targets Cse to its site of action. Recently, Carlsson et al (2006) (Carlsson *et al.*, 2006) demonstrated that the signal sequence of M protein promotes secretion at the division septum, whereas that of PrtF preferentially promotes secretion at the old pole. Thus, the possibility that the Cse signal peptide (and potentially its LysM domain) governs its secretion to mature septum is not excluded.

Within Cse protein, other regions were found to be important for the correct and specific location of the Cse protein. Indeed, depletion of the CHAP domain (Fig. 5D) or of the Var region (Fig. S1C) led to a modification of the Cse localization on *S. thermophilus* cell walls. Although we cannot exclude a direct role for these regions on cell wall attachment and/or substrate recognition, it is also possible that the CseΔvar and CseΔCHAP recombinant proteins make inadequate conformations resulting in an altered localization.

At last, not only the structure protein but also the cell wall constituents and probably its architecture possibly interfere with protein attachment. Indeed, studies of AcmA led to the conclusion that the binding of this autolysin over the entire surface is hindered by lipoteichoic acid a cell wall compound associated with glycan molecules (Steen *et al.*, 2005b).

Data from this study indicate that Cse is not involved in cell wall synthesis but only takes part in the very late stage of (or after) the cellular division to catalyse the separation of daughter cells. It demonstrates that cell separation is an active process that requires the action of dedicated cell wall hydrolases.

EXPERIMENTAL PROCEDURES

Bacterial strains, plasmids, media and growth conditions.

Bacterial strains and plasmids used in this study are listed in Table S1. *S. thermophilus* CNRZ368 and its derivatives were cultivated in milk medium, M17 (Terzaghi and Sandine, 1975) or HJL (Stingele and Mollet, 1996). Milk medium was used for strain storage, M17 for mutant generation, and Hogg Jago Lactose (HJL) for phenotypic analysis. When required, erythromycin (final concentration 2 $\mu g.ml^{-1}$) was added. *S. thermophilus* strains containing pGh9 (Maguin *et al.*, 1992) or $pNST260^{+}$ derivatives were cultivated at 30°C when plasmid self-maintenance was required and at 42°C for selection of clones with the chromosome's integrated plasmid. Phenotypic analyses were all performed at 42°C. *S. thermophilus* CNRZ368Δcse mutant was cultured in HJL at 42°C and was used (*i*) as a substrate in renaturing SDS-PAGE and (*ii*) to prepare cell-wall extracts for the zymography assays. *E. coli* strains were grown in Luria-bertani (LB) medium (Sambrook *et al.*, 1989) at 37°C with shaking. When required erythromycin or ampicillin was added to a final concentration of 150 µg/ml. *E. coli* EC101 (Leenhouts, 1995) was used as a host of recombinant plasmids derived from pGh9. *E. coli* strain DH5α was used as a host of pET15b derivatives, and *E. coli* strain BL21(DE3) (Stratagene) was used as a host to overexpress the $LysM_{Cse}$ and CHAP fusion (His_6-tagged) proteins. *B. subtilis* 168 HR was cultured in LB medium at 37°C and was used to prepare cell-wall extracts for the study of (*i*) lytic activity by zymogram and (*ii*) hydrolytic activity.

DNA and RNA manipulations

Plasmids and primers used in this study are listed in Table S1 and Table S2, respectively.

(i) Construction of *S. thermophilus* CNRZ368 cseΔLysM and cseΔCHAP mutant strains.

The LysM and the CHAP modules of the *cse* gene were deleted by allelic replacement as previously described (Thibessard *et al.*, 2004). To make deletions, the two regions flanking the LysM or CHAP

domains were independently amplified by PCR using the following primers pairs: del_lysME5'/del_lysMI5' and del_lysMI3'/del_lysME3' or del_CHAPE5'/del_CHAPI5' and del_CHAPI3'/del_CHAPE3', respectively (Table S2). The PCR products were digested by appropriate restriction enzymes, joined together and ligated with the plasmid pGh9 (Maguin *et al.*, 1992). The ligation products were used to transform *E. coli* EC101. After transformation of *S. thermophilus* with the recombinant plasmid, deleted mutants displaying an *Eco*RI restriction site replacing 459 pb of the LysM module or 318 bp of the CHAP module were selected. Deletion mutants were checked by PCR, Southern hybridization and sequencing (data not shown).

(ii) cseΔLysM and cseΔCHAP complementation.

The complementation of cseΔlysM or cseΔCHAP mutants was carried out by inserting the pNST260+::*cse* plasmid in their chromosome as previously described (Borges *et al.*, 2005).

(iii) RNA extraction and RT-PCR experiments

Total RNA was isolated from bacterial cultures according to the protocol described earlier (Kieser *et al.*, 2000). The quantity and quality of the RNA samples were verified by agarose gel electrophoresis and by measuring their absorbance at 260 and 280 nm. Isolated RNAs were stored at -80°C. Reverse transcription was performed according to the manufacturer's instructions (MMLV-reverse transcriptase, Fermentas). RNA samples isolated from *S. thermophilus* cultures were used for semi-quantitative RT-PCR analysis of the *cse* and *gyrA* transcript levels followed by separation of the PCR products on 1.5% gel agarose electrophoresis and quantitation using Quantity One software (Bio-Rad).

(iv) Construction of the pET15b::lysM$_{cse}$ and pET15b::chap plasmids for LysM$_{Cse}$- and CHAP-His$_6$-tagged proteins overexpression.

S. thermophilus CNRZ368 DNA fragments encoding (i) the 5' end of cse including the cell wall-binding LysM module (from 1 to 549 bp) and (ii) the catalytic CHAP module (from 1021 to

1383 bp) of *cse* were amplified by PCR. The amplified DNA fragments were purified, double digested with *Nde*I and *Bam*HI, repurified, and fused in-frame to the 3'end His_6-tagged of pET15b (Novagen), generating the pET15b::$lysM_{cse}$ and pET15b::chap plasmids, respectively (Table S1). The in-frame fusion was confirmed by DNA sequencing.

Overexpression, purification of His_6-tagged proteins and western blotting.

Expression of the His_6-tagged proteins was induced in *E. coli* BL21(DE3) containing pET15::$lysM_{Cse}$ or pET15b::chap by adding IPTG (to 1 mM final concentration) at OD_{600} = 0.5 for 4h at 28°C. For extraction, cells were harvested by centrifugation and disrupted on ice with a microtip of Sonifier 250 (Branson Ultrasonics). The soluble fraction containing the recombinant protein was collected by centrifugation at 14,000 rpm for 30 min at 4°C. The His_6-tagged proteins were purified by a HiTrap chelating HP column according to the manufacturer's instructions (5ml, Amersham Biosciences). The $LysM_{Cse}$- and CHAP-His_6-tagged proteins have a predicted molecular mass of 21.5 kDa and 15.1 kDa, respectively. The purity of the His_6-tagged proteins was confirmed by SDS-15% [wt/vol] polyacrylamide gel electrophoresis (PAGE) and was estimated >96% by Quantity One software (Bio-Rad). The $LysM_{Cse}$-His_6-tagged protein was used for antibodies generation; the CHAP-His_6-tagged protein was used to demonstrate Cse enzymatic properties.

For Western blotting, proteins were transferred onto PVDF membrane (Roche) using a semi-dry blotting system (Bio-Rad) following standard protocols (Towbin *et al.*, 1992). To control the presence of the His-tag on the fusion proteins, immunodetection assays were performed using rabbit IgG against RGS-His tag (Qiagen, at dilution 1:2000). The ECL Western blotting detection was done according to the manufacturer's instructions (Roche) and visualized by FluorS'max (Bio-Rad).

Cse immunolocalization.

(i) Production of anti-LysM$_{Cse}$ antibodies.

Polyclonal anti-LysM$_{Cse}$ were obtained from New Zealand White Rabbit inoculated with a mixture of 500 µg of purified LysM$_{Cse}$-His$_6$-tagged protein and Freund's complete adjuvant (Sigma-Aldrich) followed by booster two times with LysM$_{Cse}$-His$_6$-tagged protein and incomplete adjuvant every three weeks. The purified LysM$_{Cse}$-His$_6$-tagged protein was separated by SDS-15% [wt/vol] polyacrylamide gel, cut from the gel, fragmented and used for immunization. The specificity of the LysM$_{Cse}$ antibodies was verified on the purified LysM$_{Cse}$-His$_6$-tagged protein (at dilution 1:10,000) and *S. thermophilus* total proteins extract (at dilution 1:5000) by Western blotting analysis. In the soluble fraction of *S. thermophilus* CNRZ368 cells extract, one approximately 45.5 kDa band compatible with Cse molecular mass without its signal peptide (theorical molecular mass with signal peptide, 48.5 kDa) was detected with polyclonal anti-LysM$_{Cse}$ antibodies (data not shown). No band was discovered in *S. thermophilus* CNRZ368Δcse mutant cells extract, used as a negative control (data not shown).

(ii) Preparation of *S. thermophilus* samples for Cse immunolocalization.

After overnight growth at 42°C in HJL medium, samples (2 ml) of *S. thermophilus* were pelleted by centrifugation (3,000 rpm for 20 min at 4°C) and washed two times with 2 ml phosphate buffered saline (81 mM NaCl, 1.62 mM KCl, 0.9 mM KH_2PO_4, 4.8 mM K_2HPO_4 [pH 7.2]; PBS buffer). The cell pellets were resuspended in 2 ml PBS buffer and fixed by addition of 4% [vol/vol] final concentration paraformaldehyde and 0.2% [vol/vol] final concentration glutaraldehyde for 3 h of incubation on ice. Cells were harvested by centrifugation and washed four times in 2 ml PBS buffer containing 0.05 M glycine. Cells were resuspended in 1 ml PBS buffer. A sample of 100 µl was centrifugated and resuspended in 50 µl PBS buffer containing polyclonal anti-LysM$_{Cse}$ primary antibodies and incubated for 12 h at 4°C with gentle rolling. After washing, cells were resuspended in 50 µl of PBS buffer containing Alexa fluor 488-conjugated anti-rabbit IgG antibodies (1:400)

(Molecular-Probes) and observed by Fluorescence Microscopy. For Transmission Electron Microscopy (TEM), cells were resuspended in 50 µl of PBS buffer containing anti-rabbit IgG conjugated with 10 nm colloidal gold secondary antidodies (1:50) (Sigma-Aldrich). The fluorochrome calcofluor (Sigma-Aldrich) was used on *S. thermophilus* cells with a 0.01% [wt/vol] solution to reveal peptidoglycan.

(iii) Microscopy.

Immunofluorescence microscopy was performed with a Bio-Rad LRC Radiance 2100 (Elexience, Paris, France) confocal laser scanning microscope (CLSM), attached to Nikon TE2000-U inverted microscope, using an excitation at 488 nm from 100 mW argon ion laser and appropriate barrier filters. Cells were observed through x60 Nikon immersion oil plan apo (NA 1.40). Images were contrast enhanced in Adobe Photoshop (Adobe Systems Inc., Mountain View, USA). A sample of the bacterial cell suspension was deposited onto formvar carbon-coated copper nickel grids. Cells were examined with a Zeiss 902A transmission electron microscope at 80kV (magnification x 20,000 or x 30,000). *S. thermophilus* chaining phenotypes were observed with a Nikon OPTIPHOT microscope mounted with phase-contrast equipment "Ph". Cells were photographed with a Nikon coolpix 5400 digital camera.

Cell wall hydrolase activity.

(i) SDS-PAGE and zymography.

Sodium dodecyl sulfate-polyacrylamide gel electrophoresis (SDS-PAGE) were carried out as previously described with a protean II minigel system (Bio-Rad). Zymograms were performed with 15% [wt/vol] polyacrylamide separating gels containing either lyophilized of autoclaved cells (from *M. lysodeikticus* ATCC4698 (Sigma, 0.2% [wt/vol]) or from *S. thermophilus* CNRZ368Δcse mutant (0.4% [wt/vol]) or purified peptidoglycan 0.08% [wt/vol] (from *S. thermophilus* CNRZ368Δcse mutant or *B. subtilis*). Peptidoglycan from *S. thermophilus* and *B. subtilis* 168 HR vegetative cells were prepared as described previously (Courtin *et al.*, 2006; Meyrand *et al.*, 2007).

411 After electrophoresis, gels were washed two times for 30 min. in 3% [vol/vol] Triton X-100 and
412 then incubated in renaturation buffer overnight at 30°C. Proteins renaturation was performed with:
413 25 mM sodium citrate/ 50 mM sodium phosphate (Huard *et al.*, 2003) or 50 mM KH_2PO_4 buffer
414 containing 0.2% [vol/vol] Triton X-100 at pH 3 to 7. The gels were stained with 0.1% [wt/vol]
415 methylene blue in 0.01% [wt/vol] KOH for 4 h at room temperature and destained in deionized
416 H_2O. Gel images were generated with GS-800 Calibrated Densitometer Scanner (Bio-Rad).
417
418 **(ii) Determination of CHAP cell wall hydrolytic specificity.**
419 Peptidoglycan from *B. subtilis* 168 HR and *S. thermophilus* was extracted as described previously
420 (Meyrand *et al.*, 2007). *B. subtilis* peptidoglycan (4 mg) was incubated overnight at 30°C with
421 purified CHAP-His_6-tagged protein (500 µg) in a final volume of 500 µl buffer (25 mM sodium
422 citrate/ 50 mM sodium phosphate containing 0.2% Triton X-100 at pH 4.0). The sample was boiled
423 for 3 min to stop the reaction and then centrifuged at 14,000 g for 15 min. The insoluble material as
424 well as half of the soluble fraction, both recovered after incubation with CHAP-His_6-tagged protein,
425 were further treated with mutanolysin (2,500 $U.ml^{-1}$) overnight at 37°C. A control digest of
426 *B. subtilis* peptidoglycan was obtained by mutanolysin digestion as described (Courtin *et al.*, 2006).
427 The soluble muropeptides obtained after the digestions were reduced with sodium borohydride and
428 separated by reverse phase HPLC using a Hypersil ODS column (C18, 250 x 4.6 mm; 5 µm;
429 ThermoHypersil-Keystone) at 50°C using ammonium phosphate buffer and a methanol linear
430 gradient as described previously (Atrih *et al.*, 1999; Courtin *et al.*, 2006). Peaks were analysed
431 without desalting by matrix-assisted laser desorption ionization time-of-flight (MALDI-TOF) mass
432 spectrometry with a Voyager DE STR mass spectrometer (Applied Biosystems) as described
433 previously (Courtin *et al.*, 2006).
434 *S. thermophilus* peptidoglycan was digested with mutanolysin overnight at 37°C and the
435 resulting soluble muropeptides were reduced and separated by RP-HPLC as described previously
436 (Hebert *et al.*, 2007). Three muropeptides were collected, dried in a Speed-vac concentrator under
437 vacuum. The purified muropeptides were incubated with 50 µg of purified CHAP-His_6-tagged

438 protein in a total volume of 200 µl in the conditions described above for *B. subtilis* peptidoglycan.
439 The reaction products were then analyzed by RP-HPLC and MALDI-TOF mass spectrometry as
440 described above.
441

ACKNOWLEDGMENTS

This study is supported by grants from the Ministère de l'Education Nationale de l'Enseignement Supérieur et de la Recherche.

We thank Amand Chesnel for polyclonal antibodies production and Nicolas Carraro for RT-PCR experiments.

REFERENCES

Atrih, A., Bacher, G., Allmaier, G., Williamson, M.P., and Foster, S.J. (1999) Analysis of peptidoglycan structure from vegetative cells of *Bacillus subtilis* 168 and role of PBP 5 in peptidoglycan maturation. *J Bacteriol* **181**: 3956-3966.

Baker, J.R., Liu, C., Dong, S., and Pritchard, D.G. (2006) Endopeptidase and glycosidase activities of the bacteriophage B30 lysin. *Appl Environ Microbiol* **72**: 6825-6828.

Biswas, I., Gruss, A., Ehrlich, S.D., and Maguin, E. (1993) High-efficiency gene inactivation and replacement system for gram-positive bacteria. *J Bacteriol* **175**: 3628-3635.

Borges, F., Layec, S., Thibessard, A., Fernandez, A., Gintz, B., Hols, P., Decaris, B., and Leblond-Bourget, N. (2005) *cse*, a Chimeric and variable gene, encodes an extracellular protein involved in cellular segregation in *Streptococcus thermophilus*. *J Bacteriol* **187**: 2737-2746.

Borges, F., Layec, S., Fernandez, A., Decaris, B., and Leblond-Bourget, N. (2006) High genetic variability of the *Streptococcus thermophilus cse* central part, a repeat rich region required for full cell segregation activity. *Antonie Van Leeuwenhoek* **90**: 245-255.

Bourgeois, I., Camiade, E., Biswas, R., Courtin, P., Gibert, L., Gotz, F., Chapot-Chartier, M.P., Pons, J.L., and Pestel-Caron, M. (2009) Characterization of AtlL, a bifunctional autolysin of *Staphylococcus lugdunensis* with *N*-acetylglucosaminidase and *N*-acetylmuramoyl-l-alanine amidase activities. *FEMS Microbiol Lett* **290**: 105-113.

Buist, G., Kok, J., Leenhouts, K.J., Dabrowska, M., Venema, G., and Haandrikman, A.J. (1995) Molecular cloning and nucleotide sequence of the gene encoding the major peptidoglycan hydrolase of *Lactococcus lactis*, a muramidase needed for cell separation. *J Bacteriol* **177**: 1554-1563.

Buist, G., Steen, A., Kok, J., and Kuipers, O.P. (2008) LysM, a widely distributed protein motif for binding to (peptido)glycans. *Mol Microbiol* **68**: 838-847.

Calamita, H.G., Ehringer, W.D., Koch, A.L., and Doyle, R.J. (2001) Evidence that the cell wall of *Bacillus subtilis* is protonated during respiration. *Proc Natl Acad Sci U S A* **98**: 15260-15263.

474 Carlsson, F., Stalhammar-Carlemalm, M., Flardh, K., Sandin, C., Carlemalm, E., and Lindahl, G.
475 (2006) Signal sequence directs localized secretion of bacterial surface proteins. *Nature* **442**:
476 943-946.
477 Chia, J.S., Chang, L.Y., Shun, C.T., Chang, Y.Y., Tsay, Y.G., and Chen, J.Y. (2001) A 60-
478 kilodalton immunodominant glycoprotein is essential for cell wall integrity and the
479 maintenance of cell shape in *Streptococcus mutans*. *Infect Immun* **69**: 6987-6998.
480 Courtin, P., Miranda, G., Guillot, A., Wessner, F., Mezange, C., Domakova, E., Kulakauskas, S.,
481 and Chapot-Chartier, M.P. (2006) Peptidoglycan structure analysis of *Lactococcus lactis*
482 reveals the presence of an L,D-carboxypeptidase involved in peptidoglycan maturation. *J*
483 *Bacteriol* **188**: 5293-5298.
484 De Las Rivas, B., Garcia, J.L., Lopez, R., and Garcia, P. (2002) Purification and polar localization
485 of pneumococcal LytB, a putative endo-beta-*N*-acetylglucosaminidase: the chain-dispersing
486 murein hydrolase. *J Bacteriol* **184**: 4988-5000.
487 Donovan, D.M., Foster-Frey, J., Dong, S., Rousseau, G.M., Moineau, S., and Pritchard, D.G. (2006)
488 The cell lysis activity of the *Streptococcus agalactiae* bacteriophage B30 endolysin relies on
489 the cysteine, histidine-dependent amidohydrolase/peptidase domain. *Appl Environ*
490 *Microbiol* **72**: 5108-5112.
491 Eckert, C., Lecerf, M., Dubost, L., Arthur, M., and Mesnage, S. (2006) Functional analysis of AtlA,
492 the major *N*-acetylglucosaminidase of *Enterococcus faecalis*. *J Bacteriol* **188**: 8513-8519.
493 Fukushima, T., Afkham, A., Kurosawa, S., Tanabe, T., Yamamoto, H., and Sekiguchi, J. (2006) A
494 new D,L-endopeptidase gene product, YojL (renamed CwlS), plays a role in cell separation
495 with LytE and LytF in *Bacillus subtilis*. *J Bacteriol* **188**: 5541-5550.
496 Garcia, P., Gonzalez, M.P., Garcia, E., Lopez, R., and Garcia, J.L. (1999) LytB, a novel
497 pneumococcal murein hydrolase essential for cell separation. *Mol Microbiol* **31**: 1275-1281.
498 Hebert, L., Courtin, P., Torelli, R., Sanguinetti, M., Chapot-Chartier, M.P., Auffray, Y., and
499 Benachour, A. (2007) *Enterococcus faecalis* constitutes an unusual bacterial model in
500 lysozyme resistance. *Infect Immun* **75**: 5390-5398.

Heidrich, C., Templin, M.F., Ursinus, A., Merdanovic, M., Berger, J., Schwarz, H., de Pedro, M.A., and Holtje, J.V. (2001) Involvement of *N*-acetylmuramyl-L-alanine amidases in cell separation and antibiotic-induced autolysis of *Escherichia coli*. *Mol Microbiol* **41**: 167-178.

Huard, C., Miranda, G., Wessner, F., Bolotin, A., Hansen, J., Foster, S.J., and Chapot-Chartier, M.P. (2003) Characterization of AcmB, an *N*-acetylglucosaminidase autolysin from *Lactococcus lactis*. *Microbiology* **149**: 695-705.

Ishikawa, S., Hara, Y., Ohnishi, R., and Sekiguchi, J. (1998) Regulation of a new cell wall hydrolase gene, *cwlF*, which affects cell separation in *Bacillus subtilis*. *J. Bacteriol.* **180**: 2549-2555.

Kajimura, J., Fujiwara, T., Yamada, S., Suzawa, Y., Nishida, T., Oyamada, Y., Hayashi, I., Yamagishi, J., Komatsuzawa, H., and Sugai, M. (2005) Identification and molecular characterization of an *N*-acetylmuramyl-L-alanine amidase Sle1 involved in cell separation of *Staphylococcus aureus*. *Mol Microbiol* **58**: 1087-1101.

Kieser, T., Bibb, M.J., Buttner, M.J., Chater, K.F., and Hopwood, D.A. (2000) Practical *Streptomyces* genetics. Norwich, United Kingdom.

Kunst, F., Ogasawara, N., Moszer, I., Albertini, A.M., Alloni, G., Azevedo, V., Bertero, M.G., Bessieres, P., Bolotin, A., Borchert, S., Borriss, R., Boursier, L., Brans, A., Braun, M., Brignell, S.C., Bron, S., Brouillet, S., Bruschi, C.V., Caldwell, B., Capuano, V., Carter, N.M., Choi, S.K., Codani, J.J., Connerton, I.F., Danchin, A., and et al. (1997) The complete genome sequence of the gram-positive bacterium *Bacillus subtilis*. *Nature* **390**: 249-256.

Layec, S., Decaris, B., and Leblond-Bourget, N. (2008a) Characterization of proteins belonging to the CHAP-related superfamily within the *Firmicutes*. *J Mol Microbiol Biotechnol* **14**: 31-40.

Layec, S., Decaris, B., and Leblond-Bourget, N. (2008b) Diversity of *Firmicutes* peptidoglycan hydrolases and specificities of those involved in daughter cell separation. *Res Microbiol* **159**: 507-515.

Leenhouts, K. (1995) Integration strategies and vectors. *Dev Biol Stand* **85**: 523-530.

Llull, D., Lopez, R., and Garcia, E. (2006) Skl, a novel choline-binding *N*-acetylmuramoyl-L-alanine amidase of *Streptococcus mitis* SK137 containing a CHAP domain. *FEBS Lett* **580**: 1959-1964.

Maguin, E., Duwat, P., Hege, T., Ehrlich, D., and Gruss, A. (1992) New thermosensitive plasmid for gram-positive bacteria. *J Bacteriol* **174**: 5633-5638.

Margot, P., Wahlen, M., Gholamhoseinian, A., Piggot, P., and Karamata, D. (1998) The *lytE* gene of *Bacillus subtilis* 168 encodes a cell wall hydrolase. *J. Bacteriol.* **180**: 749-752.

Margot, P., Pagni, M., and Karamata, D. (1999) *Bacillus subtilis* 168 gene *lytF* encodes a gamma-D-glutamate-meso-diaminopimelate muropeptidase expressed by the alternative vegetative sigma factor, sigmaD. *Microbiology* **145 (Pt 1)**: 57-65.

Mattos-Graner, R.O., Porter, K.A., Smith, D.J., Hosogi, Y., and Duncan, M.J. (2006) Functional analysis of glucan binding protein B from *Streptococcus mutans*. *J Bacteriol* **188**: 3813-3825.

Meyrand, M., Boughammoura, A., Courtin, P., Mezange, C., Guillot, A., and Chapot-Chartier, M.P. (2007) Peptidoglycan *N*-acetylglucosamine deacetylation decreases autolysis in *Lactococcus lactis*. *Microbiology* **153**: 3275-3285.

Morlot, C., Zapun, A., Dideberg, O., and Vernet, T. (2003) Growth and division of *Streptococcus pneumoniae*: localization of the high molecular weight penicillin-binding proteins during the cell cycle. *Mol Microbiol* **50**: 845-855.

Navarre, W.W., Ton-That, H., Faull, K.F., and Schneewind, O. (1999) Multiple enzymatic activities of the murein hydrolase from staphylococcal phage phi11. Identification of a D-alanyl-glycine endopeptidase activity. *J Biol Chem* **274**: 15847-15856.

Nelson, D., Schuch, R., Chahales, P., Zhu, S., and Fischetti, V.A. (2006) PlyC: a multimeric bacteriophage lysin. *Proc Natl Acad Sci U S A* **103**: 10765-10770.

Ng, W.L., Kazmierczak, K.M., and Winkler, M.E. (2004) Defective cell wall synthesis in *Streptococcus pneumoniae* R6 depleted for the essential PcsB putative murein hydrolase or the VicR (YycF) response regulator. *Mol Microbiol* **53**: 1161-1175.

554 Ohnishi, R., Ishikawa, S., and Sekiguchi, J. (1999) Peptidoglycan hydrolase LytF plays a role in cell
555 separation with CwlF during vegetative growth of *Bacillus subtilis*. *J Bacteriol* **181**: 3178-
556 3184.
557 Pritchard, D.G., Dong, S., Baker, J.R., and Engler, J.A. (2004) The bifunctional peptidoglycan lysin
558 of *Streptococcus agalactiae* bacteriophage B30. *Microbiology* **150**: 2079-2087.
559 Rashel, M., Uchiyama, J., Takemura, I., Hoshiba, H., Ujihara, T., Takatsuji, H., Honke, K., and
560 Matsuzaki, S. (2008) Tail-associated structural protein gp61 of *Staphylococcus aureus*
561 phage phi MR11 has bifunctional lytic activity. *FEMS Microbiol Lett* **284**: 9-16.
562 Reinscheid, D.J., Gottschalk, B., Schubert, A., Eikmanns, B.J., and Chhatwal, G.S. (2001)
563 Identification and molecular analysis of PcsB, a protein required for cell wall separation of
564 group B *streptococcus*. *J Bacteriol* **183**: 1175-1183.
565 Sambrook, J., Fritsch, E.F., and Maniatis, T. (1989) *Molecular cloning : a laboratory manual*.
566 Sass, P., and Bierbaum, G. (2007) Lytic activity of recombinant bacteriophage phi11 and phi12
567 endolysins on whole cells and biofilms of *Staphylococcus aureus*. *Appl Environ Microbiol*
568 **73**: 347-352.
569 Steen, A., Buist, G., Leenhouts, K.J., El Khattabi, M., Grijpstra, F., Zomer, A.L., Venema, G.,
570 Kuipers, O.P., and Kok, J. (2003) Cell wall attachment of a widely distributed peptidoglycan
571 binding domain is hindered by cell wall constituents. *J Biol Chem* **278**: 23874-23881.
572 Steen, A., Buist, G., Horsburgh, G.J., Venema, G., Kuipers, O.P., Foster, S.J., and Kok, J. (2005a)
573 AcmA of *Lactococcus lactis* is an *N*-acetylglucosaminidase with an optimal number of
574 LysM domains for proper functioning. *Febs J* **272**: 2854-2868.
575 Steen, A., Palumbo, E., Deghorain, M., Cocconcelli, P.S., Delcour, J., Kuipers, O.P., Kok, J., Buist,
576 G., and Hols, P. (2005b) Autolysis of *Lactococcus lactis* is increased upon D-alanine
577 depletion of peptidoglycan and lipoteichoic acids. *J Bacteriol* **187**: 114-124.
578 Stingele, F., and Mollet, B. (1996) Disruption of the gene encoding penicillin-binding protein 2b
579 (*pbp2b*) causes altered cell morphology and cease in exopolysaccharide production in
580 *Streptococcus thermophilus* Sfi6. *Mol Microbiol* **22**: 357-366.

581 Terzaghi, B.E., and Sandine, W.E. (1975) Improved Medium for Lactic *Streptococci* and Their
582 Bacteriophages. *Appl Microbiol* **29**: 807-813.
583 Thibessard, A., Borges, F., Fernandez, A., Gintz, B., Decaris, B., and Leblond-Bourget, N. (2004)
584 Identification of *Streptococcus thermophilus* CNRZ368 Genes Involved in Defense against
585 Superoxide Stress. *Appl Environ Microbiol* **70**: 2220-2229.
586 Towbin, H., Staehelin, T., and Gordon, J. (1992) Electrophoretic transfer of proteins from
587 polyacrylamide gels to nitrocellulose sheets: procedure and some applications. 1979.
588 *Biotechnology* **24**: 145-149.
589 Yamamoto, H., Kurosawa, S., and Sekiguchi, J. (2003) Localization of the vegetative cell wall
590 hydrolases LytC, LytE, and LytF on the *Bacillus subtilis* cell surface and stability of these
591 enzymes to cell wall-bound or extracellular proteases. *J Bacteriol* **185**: 6666-6677.
592 Yokoi, K.J., Kawahigashi, N., Uchida, M., Sugahara, K., Shinohara, M., Kawasaki, K., Nakamura,
593 S., Taketo, A., and Kodaira, K. (2005) The two-component cell lysis genes holWMY and
594 lysWMY of the *Staphylococcus warneri* M phage varphiWMY: cloning, sequencing,
595 expression, and mutational analysis in *Escherichia coli*. *Gene* **351**: 97-108.
596 Yoshimura, G., Komatsuzawa, H., Hayashi, I., Fujiwara, T., Yamada, S., Nakano, Y., Tomita, Y.,
597 Kozai, K., and Sugai, M. (2006) Identification and molecular characterization of an *N*-
598 Acetylmuraminidase, Aml, involved in *Streptococcus mutans* cell separation. *Microbiol*
599 *Immunol* **50**: 729-742.
600
601

LEGEND FIGURES

FIG. 1. RT-PCR detection of *cse* transcripts.

A. *cse* modular structure. The positions in nucleotides delimit the signal peptide (SP), the LysM cell wall-binding module, the central variable region (Var) and the catalytic CHAP module of *S. thermophilus* CNRZ368 *cse* gene. Arrows and hairpin loops symbolize putative promoters and putative rho-independent transcriptional terminators, respectively. **B.** Semi-quantitative RT-PCR assays were carried out to compare the level of expression of the different *cse* alleles (*cse*, *Δcse*, *cseΔlysM, cseΔvar* and *cseΔchap*). Semi-quantitative RT-PCR reactions were performed with *cse* locus specific primers (surlysM5' and Del_lysMI5') referred in Table S2, yielding a product of 110 bp in size. The internal housekeeping gene *gyrA* served as a reference point to detect relative difference in the integrity of individual RNA samples and was amplified using the gyrA5' and gyrA3' primers (Table S2), which yielded a product of 140 bp in size. As a negative control, all DNAse RNA samples were subjected to PCR prior to RT analysis [- RT (gyrA)]. T(-), also corresponds to a negative control, using water as a PCR matrix. As positive control [T(+)], DNA samples extracted from the culture of each strains were subjected to PCR. For semi-quantitative analysis, the density ratios of the *cse* mutant allele versus the *cse* wild-type were calculated and used as an indication for the relative expression (*cse* = 100%*; Δcse* = 0%; *cseΔlysM* = 99.3+/- 2.9%; *cseΔvar* = 94.7+/- 6.2% and *cseΔchap* = 97.2+/- 8.2%).

FIG. 2. Mutation of *cse* alters *S. thermophilus* cell separation.

A. Picture of standing HJL cultures and phase contrast microscopy of the strains. Photographs were taken after 20 h of growth at 42°C in HJL medium. Magnification, x1,000. **B.** Chain length analysis. Cells were counted in stationary phase after 20 h of growth at 42°C in HJL medium. The error bars represent standard deviations of three independent experiments. The chain length analysis of the cseΔVar mutant was reported in the following reference (Borges *et al.*, 2006).

FIG. 3. *S. thermophilus* chaining phenotype observed by transmission electron microscopy (TEM).

The Δcse mutant chaining phenotype is shown in panels A to C, that of the wild-type in D to F. Cells were visualized after 20 h of growth at 42°C in HJL medium. Arrowheads in panels C and F pointed distinct septa. Diplococcal dividing cells are characterized by the in-growth of the septum (nascent septum, a) initiated by the constriction ring located equidistant from the cell poles. The progression of the septal peptidoglycan synthesis is materialized by the further constriction of the cell walls (intermediate septum, b). At the end of the division process, diplococcal cells are held together by a thin peptidoglycan filamentous corresponding to an extension of the septum (mature septum, c). Bars = 0.5 µm.

FIG. 4. Immunolocalization of Cse on *S. thermophilus* cell surface.

The TEM pictures of the wild-type strain are shown in A to D and that of the Δcse mutant in E and F. Cells were successively probed with anti-$LysM_{Cse}$ rabbit polyclonal antibodies (A, B, C, E and F) or with preimmun serum (D) and with anti-rabbit IgG conjugated with 10 nm colloidal gold secondary antibody. The localization of Cse protein is indicated by the arrowheads pointed on gold-conjugates secondary antibodies (A to C). No labelling was observed on the negative controls (D to F). Bars = 0.1 µm.

FIG. 5. Cse localizes on *S. thermophilus* CNRZ368 mature septa.

CNRZ368 wild-type (A, B and E), cseΔLysM (C) and cseΔCHAP (D) cells are shown. Surface bound Cse and derivatives proteins were detected by immunofluorescence microscopy using anti-$LysM_{Cse}$ antibodies. Phase-contrast images (A1 to E1) and fluorescence images (A2 to B2 and E2 to E4) of the bacterial cells in the same field are shown. The arrowheads pointed mature septa. No fluorescence staining on the wild-type cell surface was observed using the preimmun serum (B2), as

653 well as on the cseΔLysM mutant cells with the anti-LyM_{Cse} antibodies (C2), as negative controls,
654 (Bars = 25 μm).
655 E2 shows a single-labeled with anti-$LysM_{Cse}$ antibodies that indicates the localization of Cse
656 exclusively on mature septa (Bars = 5 μm). E3 shows the fluorochrome calcofluor having an
657 affinity for peptidoglycan. E4 is the result double-labelled.
658
659 **FIG. 6. Cse functions as an endopeptidase.**
660 **A.** RP-HPLC analysis of the muropeptides released from *B. subtilis* cell wall after incubation with
661 mutanolysin (a) or the CHAP-His_6-tagged protein and mutanolysin (b). **B.** RP-HPLC analysis of
662 three different purified muropeptides from *S. thermophilus* (Table 1, Fig. S4) after digestion with
663 the CHAP-His_6-tagged protein. The numbers indicate the peaks analyzed by MALDI-TOF MS. The
664 molecular ions *m/z* values are indicated in Table 1. The CHAP domain activity is visible as a clear
665 hydrolysis band observed on a renaturing SDS-PAGE with 8 μg of CHAP-His_6-tagged protein in
666 gel containing 0.08% [wt/vol] *B. subtilis* HR168 or *S. thermophilus* CNRZ368Δcse cell-wall as
667 substrate.
668 The percentage of monomers corresponds to the sum of the area of the peaks corresponding to
669 monomers over the sum of the areas of all peaks. The same was done for dimers and trimers. The
670 percentage of each peak was calculated as the ratio of the peak area over the sum of areas of all the
671 peaks identified by RP-HPLC.
672 Schematic structure of *S. thermophilus* cell-wall is illustrated. Arrow indicates the cleavage site of
673 the CHAP-His_6-tagged protein. GlcNAc, *N*-acetylglucosamine; MurNAc, *N*-acetylmuramic acid.
674
675 **FIG. S1. Immunolocalization of Cse protein derivaties on the cell surface of *S. thermophilus*.**
676 *S. thermophilus* CNRZ368 cells of the Δcse (A), the cseΔCHAP (B) and the cseΔVar (C and D)
677 mutants are shown. Cells were vizualized with a laser scanning confocal microscope. Phase-constrat
678 images (A1 to D1) and fluorescence images (A2 to D2) of the bacterial cells are shown in the same

679 field. No fluorescence was detected on negative controls: Δcse cells with anti-$LysM_{Cse}$ antibodies
680 (A2); from cseΔCHAP to cseΔvar cells with preimmun serum (B2 and D2). C2 indicates the
681 localization of Cse derivative protein using the $LysM_{Cse}$ antibodies. (Bars = 25 μm)
682
683 **FIG. S2. Overexpression, purification, western-blotting and lytic activity of the CHAP-His_6-**
684 **tagged protein.**
685 SDS-15% polyacrylamide gel with Coomassie brilliant blue staining, Western blot obtained using
686 RGS-His-tag antibodies raised against CHAP-His_6-tagged protein and Cell wall hydrolytic activity
687 of the CHAP-His_6-tagged protein in renaturing SDS-15% polyacrylamide gel containing 0.08%
688 [wt/vol] *B. subtilis* 168 HR or *S. thermophilus* CNRZ368Δcse peptidoglycan as substrate.
689 Renaturing buffer contains 0.2% TritonX-100. The CHAP-His_6-tagged protein activity is visible as
690 cleaning zones in the gel (lanes 3, 4 and 5). Lanes 1 and 2, cell extract and supernatant of *E. coli*
691 BL21(DE3) containing pET15b. Lanes 3 and 4, cell extract and supernatant of *E. coli* BL21(DE3)
692 containing pET15b::chap. Lane 5, purified CHAP-His_6-tagged protein. Lane MM, the molecular
693 masses of standard proteins. The arrow indicates the position of purified CHAP-His_6-tagged
694 protein.
695
696 **FIG. S3. Schematic structure of the muropeptides from *S. thermophilus* obtained after**
697 **mutanolysin digestion or after CHAP-His6-tagged protein and mutanolysin digestion.**
698 Numbers peaks on the chromatograms presented in Fig. 6 and Table 1.
699
700 **FIG. S4. Purity of *Streptococcus thermophilus* muropeptides.**
701 Chromatogram of the three muropeptides from *S. thermophilus* peptidoglycan before CHAP-His_6-
702 protein digestion. The molecular ions *m/z* values of peaks 8, 9 and 10 are indicated in Table 1 and
703 their structures are illustrated in Fig. S3.
704
705

706

707 **Table S1.** Bacterial strains and plasmids used in this study.

Strain or plasmid	Genotype/phenotype/ source	Origin/reference
***S. thermophilus* strains**		
CNRZ368	Wild-type; isolated from yogurt.	INRA-CNRZ, strain collection, France
CNRZ368Δcse	Derivative of CNRZ368 carrying a 1359 bp deletion in the *cse* gene	(Borges *et al.*, 2005)
CNRZ368cseΔLysM	Derivative of CNRZ368 carrying a 459 bp deletion in the cse LysM Module	This study
CNRZ368cseΔVar	Derivative of CNRZ368 carrying a 345 bp deletion in the var- *cse* Region	(Borges *et al.*, 2005)
CNRZ368cseΔCHAP	Derivative of CNRZ368 carrying a 318 bp deletion in the *cse* CHAP Module	This study
E. coli *strains*		
EC101	*supE hsd-5 thi Δ(lac-proAB)* F'*(traD6 proAB*$^+$ *lacI*^{q} *lacZΔM15) repA*$^+$, derivative of TG1 strain (Sambrook *et al.*, 1989)	(Leenhouts, 1995; Sambrook *et al.*, 1989)
DH5α	F$^-$, *end*A1, *gyr*A96, *thi*-1, *hsd*R17(r_K^-,m_K^+), *sup*E44, *rel* A1, *M15, Δ (lacZYA-argF),U169*	(Sambrook *et al.*, 1989)
BL21(DE3)	*E. coli* B, F$^-$, *dcm, ompT, hsd*S($r_B^-m_B^-$), *gal*λ(DE3)	Stratagene
B. subtilis		
168 HR	*trpC2*	(Kunst *et al.*, 1997)
Plasmids		
pGh9	Thermosensitive plasmid, used for gene replacement; Ery^R	(Biswas *et al.*, 1993; Maguin *et al.*, 1992)
pGh9 ::cseΔlysM	Derivative of pGh9 carrying a 1098 bp for LysM deletion	This study
pGh9 ::cseΔCHAP	Derivative of pGh9 carrying a 924 bp for CHAP deletion	This study
pNST260+	Derivative of pGh9 carrying a *int* gene coding a integrase and an *attI* from ICE*St*1, specific-site of recombinaison	G. Guédon, personal communication
pNST260+ ::cse	pNST260+ with CNRZ368 *cse* gene, its putative promoter and terminator	(Borges *et al.*, 2005)
pET15b	Expression vector for N-terminal His_6-tagged fusion; Amp^R	Novagen
pET15b :: $lysM_{cse}$	Derivative of pET15b carrying a 549 bp insert coding a $LysM_{Cse}$ His_6-tagged protein	This study
pET15b :: chap	Derivative of pET15b carrying a 369 bp insert coding a CHAP His_6-tagged protein	This study

708

709

710 **Table S2.** Primers used in this study.

Name	Sequence (5'to 3')[a]	Restriction sites
Construction of *S. thermophilus* cseΔlysM mutant		
Del_lysME5'	CCC CCC CC**A AGC TT**A CAA GAT CAG TTT GGA AC	*Hin*dIII
Del_lysMI5'	CCC CCC **GAA TTC** ACG TGC TGT CCA GTG A	*Eco*RI
Del_lysMI3'	CCG **GAA TTC** GAT GCT ATT GAT CAT GTT AC	*Eco*RI
Del_lysME3'	CCC C**CT GCA G**TC GAT ATG TAT TAG GAG TT	*Pst*I
Construction of *S. thermophilus* cseΔchap mutant		
Del_CHAPE5'	CCC CC**A AGC TT**G ATG CTA TTG ATG CTA TTG ATC ATG TTA	*Hin*dIII
Del_CHAPI5'	CCG **GAA TTC** AGT TGA TGC ATA TTC GTA T	*Eco*RI
Del_CHAPI3'	CCC CCC **GAA TTC** ATT TAT CCA TAA TGA GTA CA	*Eco*RI
Del_CHAPE3'	CCC CCC **CTG CAG** CCT GTG GTT GAA G	*Pst*I
Construction of pET15b::lysM$_{cse}$		
surlysM5'	CCC CCC C**CA TAT G**TT ATC AAA ATC TAA AAC	*Nde*I
surlysM3'	CCC C**GG ATC C** TT AAG CTG GAG TAT CTG ATG C	*Bam*HI
Construction of pET15b::chap		
surchap5'	CCC CCC C**CA TAT G** CT AGC AGC TAC ATA CGA ATA	*Nde*I
surchap3'	CCC C**GG ATC C**TT ATG GAT AAA TAT AAT ATA CAG AA	*Bam*HI
***gyrA* gene expression**		
gyrA5'	GATGCCGTTAAATTGATGAT	/
gyrA3'	GAGCCTTTACCAGTTTCGTA	/

711

712 [a] Restriction sites are in boldface and underlined.

713 **Table 1**: Observed *m/z* values for sodiated molecular ions of muropeptides obtained after hydrolysis
714 of *B. subtilis* and *S. thermophilus* peptidoglycan.

715

Peak [a]	[M+Na]+ observed	Muropeptide identification[b]
Bacillus subtilis		
1	852.3	DS-Tri (NH_2)
2	1815.7	DS-Tri-DS-Tetra (NH_2)
3	1814.7	DS-Tri (NH_2)-DS-Tetra (NH_2)
4	964.4	DS-Tetra
5	963.4	DS-Tetra (NH_2)
Streptococcus thermophilus		
6	1061.3	DS-Tetra –Ala Ala (NH_2)
7	1132.4	DS- Penta – Ala Ala (NH_2)
8	2081.9	DS- Tetra (NH_2) – Ala Ala – DS Tetra (NH_2)– Ala Ala
9	2153.0	DS- Penta (NH_2) – Ala Ala – DS Tetra (NH_2) – Ala Ala
10	3173.3	DS- Penta (NH_2) – Ala Ala – DS Tetra (NH_2) – Ala Ala – DS Tetra (NH_2) – Ala Ala

716

717 [a] Peak numbers refer to the peaks on the chromatograms presented in Fig. 6, which were analyzed
718 by mass spectrometry.

719 [b] DS, disaccharide GlcNAc-MurNAc (GlcNAc, *N*-acetylglucosamine; MurNAc, *N*-acetylmuramic
720 acid). Tri, tripeptide (L-Ala-D-γGlu-mDAP) from *B. subtilis*; Tetra, tetrapeptide (L-Ala-D-γGlu-
721 mDAP-D-Ala) from *B. subtilis* and (L-Ala-D-γGlu-L-Lys-D-Ala) from *S. thermophilus*; Penta,
722 pentapeptide (L-Ala-D-γGlu-L-Lys-D-Ala-D-Ala) from *S. thermophilus*.

723 NH_2 indicates the presence of an amidation on the peptide chain on mDAP from *B. subtilis*
724 according to (Atrih *et al.*, 1999) and most probably on D–γ-Glu from *S. thermophilus*.

725

726

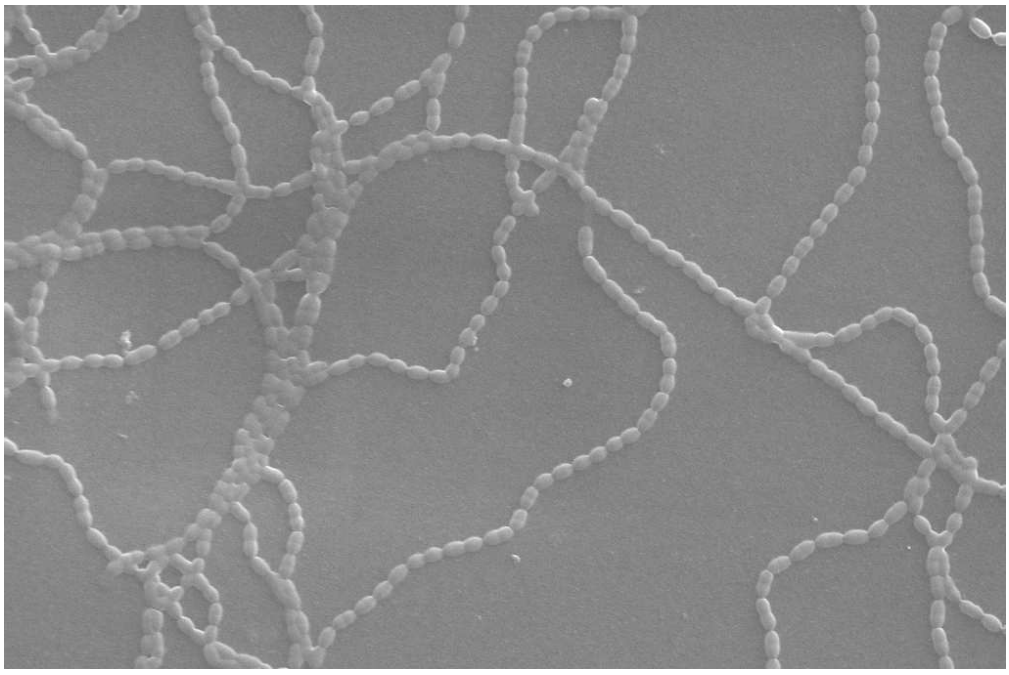

Scanning electron photograph of Streptococcus thermophilus csedeltaLysM mutant. The long chain phenotype indicates that the binding of Cse at cell surface is required for efficient cell separation.
Magnification, x 4,780
26009x17272mm (1 x 1 DPI)

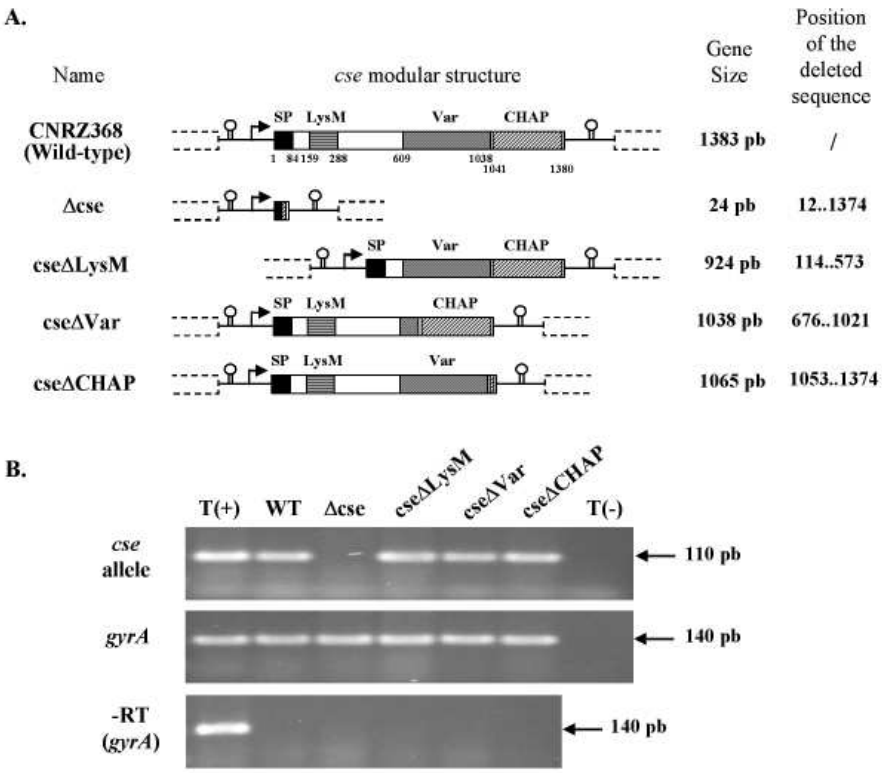

Fig. 1

FIG. 1. RT-PCR detection of cse transcripts. A. cse modular structure. The positions in nucleotides delimit the signal peptide (SP), the LysM cell wall-binding module, the central variable region (Var) and the catalytic CHAP module of S. thermophilus CNRZ368 cse gene. Arrows and hairpin loops symbolize putative promoters and putative rho-independent transcriptional terminators, respectively. B. Semi-quantitative RT-PCR assays were carried out to compare the level of expression of the different cse alleles (cse, Δcse, cseΔlysM, cseΔvar and cseΔchap). Semi-quantitative RT-PCR reactions were performed with cse locus specific primers (surlysM5' and Del_lysMI5') referred in Table S2, yielding a product of 110 bp in size. The internal housekeeping gene gyrA served as a reference point to detect relative difference in the integrity of individual RNA samples and was amplified using the gyrA5' and gyrA3' primers (Table S2), which yielded a product of 140 bp in size. As a negative control, all DNAse RNA samples were subjected to PCR prior to RT analysis [- RT (gyrA)]. T(-), also corresponds to a negative control, using water as a PCR matrix. As positive control [T(+)], DNA samples extracted from the culture of each strains were subjected to PCR. For semi-quantitative analysis, the density ratios of the cse mutant allele versus the cse wild-type were calculated and used as an indication for the relative expression (cse =100% deltacse = 0%; csedeltalysM = 99.3+/- 2.9%; csedeltavar = 94.7+/- 6.2% and csedeltachap = 97.2+/- 8.2%).
178x171mm (96 x 96 DPI)

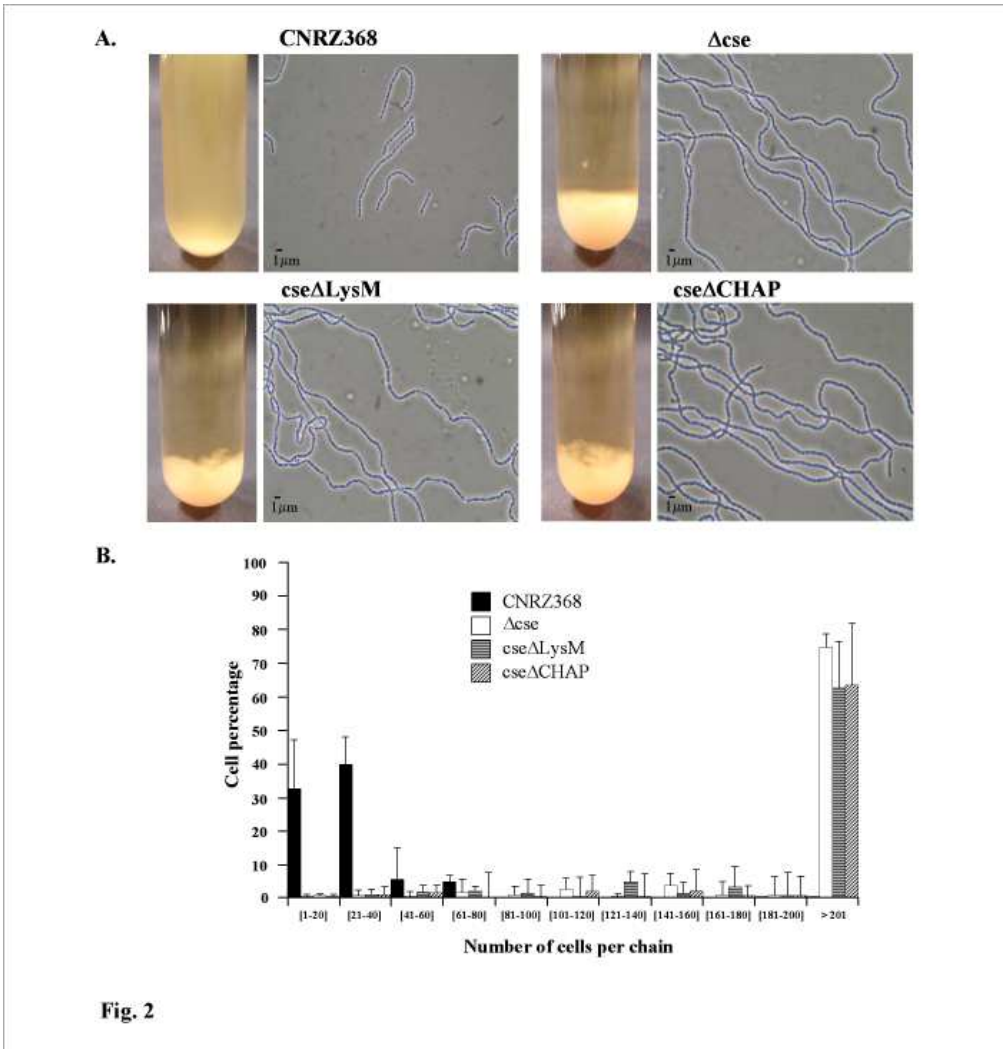

Fig. 2

FIG. 2. Mutation of cse alters S. thermophilus cell separation. A. Picture of standing HJL cultures and phase contrast microscopy of the strains. Photographs were taken after 20 h of growth at 42°C in HJL medium. Magnification, x1,000. B. Chain length analysis. Cells were counted in stationary phase after 20 h of growth at 42°C in HJL medium. The error bars represent standard deviations of three independent experiments. The chain length analysis of the csedeltaVar mutant was reported in the following reference (Borges et al., 2006).
184x193mm (96 x 96 DPI)

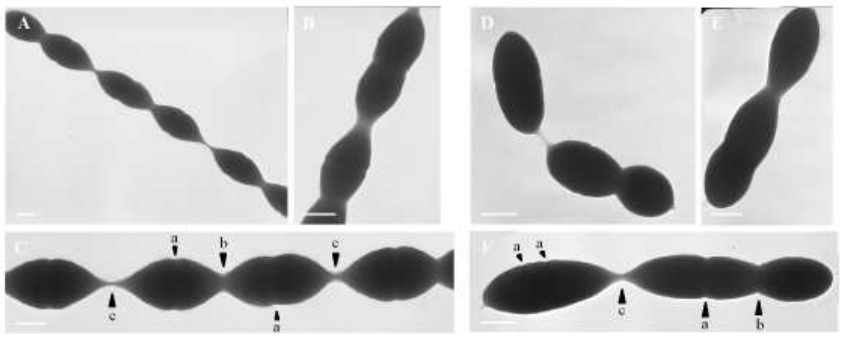

Fig. 3

FIG. 3. S. thermophilus chaining phenotype observed by transmission electron microscopy (TEM). The deltacse mutant chaining phenotype is shown in panels A to C, that of the wild-type in D to F. Cells were visualized after 20 h of growth at 42°C in HJL medium. Arrowheads in panels C and F pointed distinct septa. Diplococcal dividing cells are characterized by the in-growth of the septum (nascent septum, a) initiated by the constriction ring located equidistant from the cell poles. The progression of the septal peptidoglycan synthesis is materialized by the further constriction of the cell walls (intermediate septum, b). At the end of the division process, diplococcal cells are held together by a thin peptidoglycan filamentous corresponding to an extension of the septum (mature septum, c). Bars = 0.5 µm.
175x101mm (96 x 96 DPI)

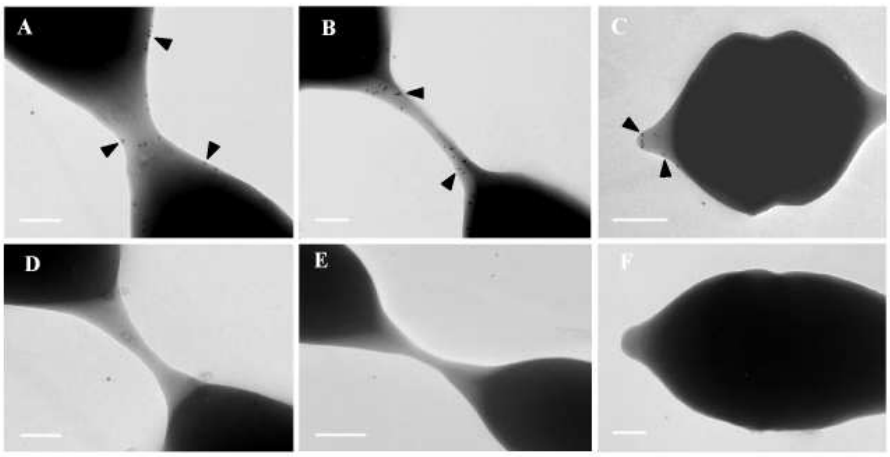

Fig. 4

FIG. 4. Immunolocalization of Cse on S. thermophilus cell surface. The TEM pictures of the wild-type strain are shown in A to D and that of the deltacse mutant in E and F. Cells were successively probed with anti-LysMCse rabbit polyclonal antibodies (A, B, C, E and F) or with preimmun serum (D) and with anti-rabbit IgG conjugated with 10 nm colloidal gold secondary antibody. The localization of Cse protein is indicated by the arrowheads pointed on gold-conjugates secondary antibodies (A to C). No labelling was observed on the negative controls (D to F). Bars = 0.1 µm.
189x127mm (96 x 96 DPI)

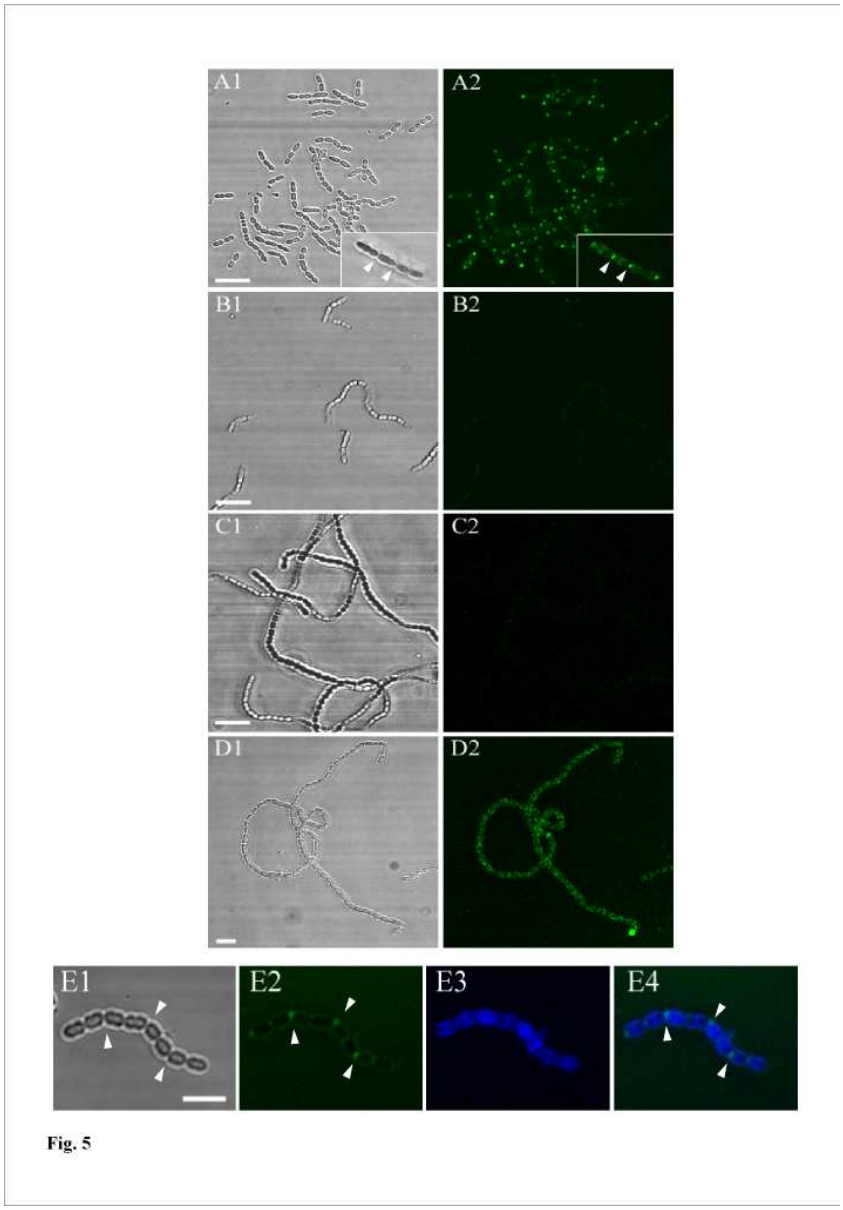

FIG. 5. Cse localizes on S. thermophilus CNRZ368 mature septa. CNRZ368 wild-type (A, B and E), csedeltaLysM (C) and csedeltaCHAP (D) cells are shown. Surface bound Cse and derivatives proteins were detected by immunofluorescence microscopy using anti-LysMCse antibodies. Phase-contrast images (A1 to E1) and fluorescence images (A2 to B2 and E2 to E4) of the bacterial cells in the same field are shown. The arrowheads pointed mature septa. No fluorescence staining on the wild-type cell surface was observed using the preimmun serum (B2), as well as on the csedeltaLysM mutant cells with the anti-LysMCse antibodies (C2), as negative controls, (Bars = 25 µm). E2 shows a single-labeled with anti-LysMCse antibodies that indicates the localization of Cse exclusively on mature septa (Bars = 5 µm). E3 shows the fluorochrome calcofluor having an affinity for peptidoglycan. E4 is the result double-labelled.
188x270mm (96 x 96 DPI)

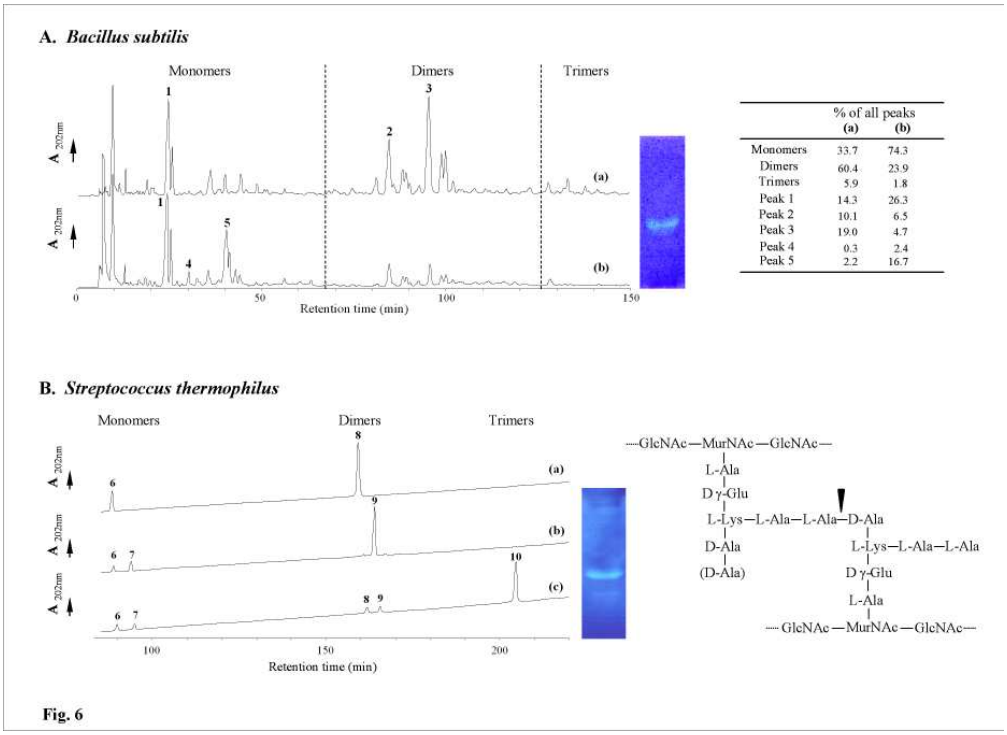

	% of all peaks (a)	(b)
Monomers	33.7	74.3
Dimers	60.4	23.9
Trimers	5.9	1.8
Peak 1	14.3	26.3
Peak 2	10.1	6.5
Peak 3	19.0	4.7
Peak 4	0.3	2.4
Peak 5	2.2	16.7

Fig. 6

FIG. 6. Cse functions as an endopeptidase. A. RP-HPLC analysis of the muropeptides released from B. subtilis cell wall after incubation with mutanolysin (a) or the CHAP-His6-tagged protein and mutanolysin (b). B. RP-HPLC analysis of three different purified muropeptides from S. thermophilus (Table 1, Fig. S4) after digestion with the CHAP-His6-tagged protein. The numbers indicate the peaks analyzed by MALDI-TOF MS. The molecular ions m/z values are indicated in Table 1. The CHAP domain activity is visible as a clear hydrolysis band observed on a renaturing SDS-PAGE with 8 µg of CHAP-His6-tagged protein in gel containing 0.08% [wt/vol] B. subtilis HR168 or S. thermophilus CNRZ368deltacse cell-wall as substrate. The percentage of monomers corresponds to the sum of the area of the peaks corresponding to monomers over the sum of the areas of all peaks. The same was done for dimers and trimers. The percentage of each peak was calculated as the ratio of the peak area over the sum of areas of all the peaks identified by RP-HPLC. Schematic structure of S. thermophilus cell-wall is illustrated. Arrow indicates the cleavage site of the CHAP-His6-tagged protein. GlcNAc, N-acetylglucosamine; MurNAc, N-acetylmuramic acid.
246x178mm (96 x 96 DPI)